3 RADIOFREQUENCY ELECTROMAGNETIC FIELDS INSIDE THE BODY

The body interacts with radiofrequency (RF) electromagnetic fields (EMFs) and the strengths of the fields inside the body are quite different from those outside.

This chapter describes the relationships between external fields to which the body is exposed and the induced fields that result inside the body. The scope is mainly restricted to studies in humans, although the methods and principles described apply equally to characterising the exposures of animals, cells and other biological structures in experimental systems.

3.1 Principles of interactions with the body

A radio frequency (RF) electromagnetic field (EMF) in air can be reflected, transmitted, refracted or scattered by a biological body. The reflected and scattered fields may proceed in directions different from that of the incident RF field, while the transmitted and refracted fields interact (are coupled) with the biological body in different ways. These interactions are strongly dependent on the frequency, waveform, and strength of the induced fields as well as the energy deposited or absorbed in the biological system. In addition, the distribution of the fields inside a biological system such as the human body is affected by the distance and location of the source with respect to the body, the anatomy, posture and the surrounding environment of the body.

3.1.1 Coupling of the body to the field

Coupling between an incident uniform (plane-wave) RF field and the human body depends only on the frequency, the direction of incidence and the polarisation of the field. Where exposure to non-uniform fields occurs, as when in close proximity to sources, the coupling also depends on the source characteristics, position and orientation with respect to the body. Source-related considerations affecting exposure, such as near and far-field regions, and mutual coupling, are discussed in Chapter 2, as are environmental considerations such as reflections and multipath propagation.

Coupling is strongly dependent on the ratio of wavelength, λ, to that of the body dimensions; therefore it is convenient to divide the RF EMF spectrum into three regions when considering physical interactions.

1. Body dimensions are small in relation to the wavelength, λ, for frequencies between 100 kHz and 10 MHz (λ > 30 m). Coupling to the body is weak, but RF energy penetrates deeply so generalised absorption occurs throughout the body tissues.

2. Body dimensions such as height and limb length become comparable with the wavelength for frequencies in the range 10 MHz to 2 GHz (30 m > λ >15 cm) so resonances can occur, giving a strong dependence between coupling and frequency and a complicated pattern of absorption in the body tissues.

3. Between 2 GHz and 300 GHz (λ < 15 cm) the wavelength is small in relation to the body tissues and coupling is characterised by small penetration into the body tissues and surface dominated absorption.

These aspects of coupling and the mechanisms giving rise to them are discussed further in Section 3.1.4.

Both direct and indirect coupling of external RF fields into the human body can occur (see next section) and result in the induction of fields and currents inside the body tissues. Dielectric and ohmic losses in the tissues lead to energy absorption and a rise in local or whole body temperature. In addition, where the exposure occurs within the reactive near-field region with respect to a source (see chapter 2) the electric and magnetic components of the incident field interact differently with the body. Hence, both quantities and their respective interactions must be determined separately and summed together in order to fully characterise the human exposure.

3.1.2 Direct and indirect effects

RF EMFs carry energy and when the body is exposed to them, some of the energy is absorbed, a *direct effect* which leads to heating of the body tissues (WHO, 1993). At frequencies below 100 kHz (and therefore not in the scope of this document), the physical quantity identifiable with most biological effects is the electric field strength in tissue, which is related to the current density. These effects are related to electrical

stimulation of tissues, but become less prominent as frequency increases and are disregarded for frequencies above 10 MHz. Generally, in the RF region (and exclusively above 10 MHz), the rate at which the body is heated is considered a more appropriate measure to assess the exposure.

Contact with a radio antenna or metallic conductor placed in a RF field can lead in some circumstances to electric shock or burn, *indirect effects* that result from current flow in the body tissues (Chatterjee, Wu & Gandhi, 1986). Shock is related to electrostimulation of tissues and burn occurs due to intense and rapid localised heating. Electrical burns follow the path of current flow through the body tissues and can be much deeper than burns that result from contact with hot objects. They can occur at points where current exits the body as well as where it enters the body.

Many factors determine the potential for electrical burn or shock including the power density, frequency of the signals, the grounding conditions, whether the structure has resonant dimensions and how much of the body is in contact with the conductor. Electrical burns can be a hazard for those working near antennas and other metallic structures either radiating or exposed to RF fields. However, they are exploited to beneficial effect in medicine where they are applied in electrosurgery.

3.1.3 Absorption of RF energy

The absorption of energy from RF EMF causes molecules to vibrate which in turn leads to heating of body tissues. This absorption (and the consequent heating) is defined by a quantity known as the specific energy absorption rate (SAR), with unit, watt per kilogram (W/kg). SAR is derived from the square of the (instantaneous) electric field strength, E, in tissue:

$$\mathrm{SAR} = \frac{1}{2}\frac{\sigma}{\rho}E^2 \qquad (3.1)$$

where σ and ρ are the conductivity (in siemens per metre, S/m) and the density (kg/m^3) of the tissue of interest. For a sinusoidally varying electric field, the factor of ½ may be omitted and the rms (root mean squared, see Chapter 2) value of the field substituted in the above equation in order to obtain the time-averaged SAR.

SAR provides a measure of the power absorbed from a radio frequency signal per kilogram of body tissue and is often used as a proxy for the amount of heating or temperature rise in the body. It may be derived at a point in time and space in the body tissues; however, it is more usual to average the quantity over time and space in some appropriate way. Whole-body SAR may be derived by averaging the quantity over all tissues of the body or localised SAR may be derived for a particular organ, tissue type or body part, e.g. by averaging over a 1 g or 10 g mass of tissue in which the maximum SAR occurs. Averaging time is relevant to thermal considerations because the heating potential of an exposure depends on how quickly a certain amount of energy can be input in relation to how quickly it can be dissipated by the body. SAR is generally averaged over a period of 6 minutes in order to derive a quantity closely related to the heating potential of absorbed RF energy (ICNIRP, 1998).

SAR cannot be measured non-invasively so it cannot be measured easily in a living system. It is therefore usually estimated from simulations using experimental or computer-based models of the living body (see section 3.2).

3.1.4 Factors affecting human exposure

3.1.4.1 Body resonance

The human body acts as an oblong mass of poorly conducting material when exposed to RF fields. It is particularly effective at absorbing RF fields under resonant conditions where the wavelength of the radiation is comparable with the dimensions of the body. Maximum coupling occurs if the incident electric field is polarized parallel to the long body axis and resonant currents flow up and down the body. The resonance occurs when the body height is approximately half a wavelength ($\lambda/2$) for an ungrounded body and nearer a quarter wavelength ($\lambda/4$) for a person standing in electrical contact with a conducting ground plane (Conil et al., 2008; Dimbylow, 2005a; Dimbylow, 1997; Kühn et al., 2009). An example set of computational results showing how SAR averaged over the whole body mass varies in relation to body height and grounding conditions is shown in Figure 3.1.

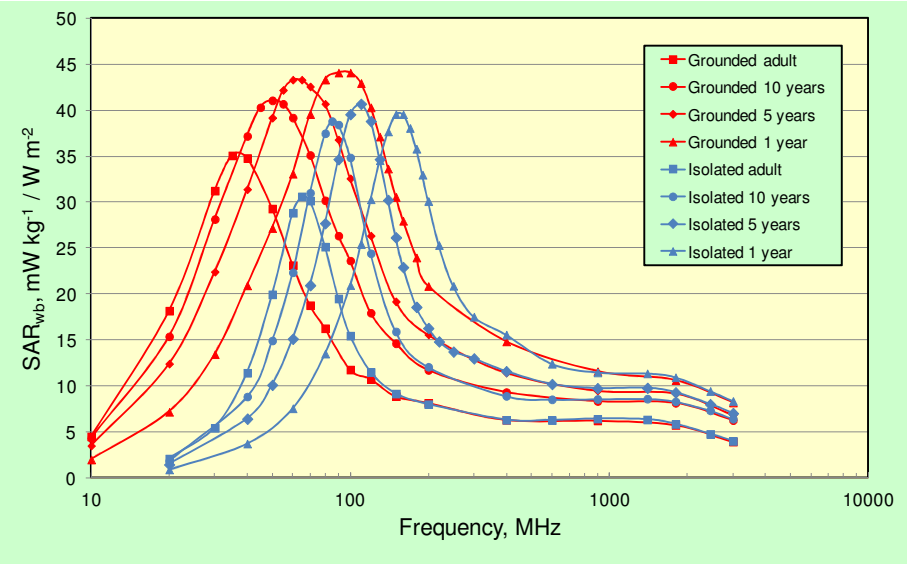

Figure 3.1. Predicted whole body SAR in typical models of the human body per unit power density of a vertically polarised plane wave incident towards the chest. The basic model is of a 73 kg, 1.76 m tall adult male standing with its arms to the side and this has been scaled to have heights/masses representative of children at different ages. Conditions are also considered where the shoes effectively form an electrical contact between the body and a conducting plane beneath it and where they provide isolation (Data from Dimbylow (2005a; 1997).

The frequency of resonance depends on the size, shape and posture of the exposed individual. It also depends on the direction from which the wave is incident and the polarisation of the incident electromagnetic field with respect to the body. In the case of a vertically polarised wave incident on the body, as shown in Figure 3.1, the resonance frequency is particularly strongly affected by the height of the exposed person and the ease with which current can flow through the feet to ground. For standing adults, the peak of this resonant absorption occurs in the frequency range of 70–80 MHz if they are electrically isolated from ground and at about half this frequency if they are electrically grounded. Smaller adults and children show the resonance at higher frequencies. In addition to whole-body resonance, it is possible for partial-body resonances to occur, e.g. in the limbs.

3.1.4.2 Exposure below body resonance

For uniform (plane wave) exposures, as frequency reduces below that of the body resonance the body acts as a short poor conductor and couples increasingly weakly to RF fields, as shown in Figure 3.1. In this region, the SAR is approximately proportional to the height of a person and to the frequency squared.

In this frequency range, the highest exposures tend to occur in practice from near-field sources (see Chapter 2) that generally have strong field gradients and are used within a few metres of the body. Under such conditions, the energy is either capacitively or inductively coupled to the body (instead of through radiation), depending on whether electric or magnetic field component is the dominant source. Examples of such exposure scenarios are with dielectric heaters and diathermy applicators where electric field source is dominant, and with inductive cooking hobs, anti-theft systems, wireless power transfer systems, and magnetic resonance imaging where the magnetic field source is dominant.

3.1.4.3 Exposures above body resonance

At frequencies above body resonance, the body acts as a dielectric[1] object that is large with respect to the wavelength and to the penetration depth (skin depth – see below) of the radiation into the body tissues. Therefore, the absorbed energy is approximately proportional to the exposed surface area of the body (Gosselin et al., 2009). In turn, whole body SAR is proportional to the ratio of exposed surface area to the body mass

[1] Dielectric materials are materials in which locally bound electric charges can be displaced in response to an externally imposed field, leading to polarisation of domains inside the material.

(Kühn et al., 2009). This is consistent with the results shown in Figure 3.1, which show that children have higher whole-body SAR than adults at frequencies around and above body resonance.

3.1.4.4 Skin depth

RF fields become less penetrating into body tissues as frequency increases so the energy they deposit in the body becomes increasingly confined to the body surface. A useful figure of merit to describe the penetration is the skin depth, a distance over which the electromagnetic field component of a wave penetrating into a material reduces to 37% of its initial value, as illustrated in Figure 3.2. The skin depth of tissues depends on their electrical permittivity[2] and conductivity. The general expression for skin depth for poor conductors (non-metals) at radio frequencies is as follows (Griffiths, 1989):

$$\delta = (\frac{1}{\omega})\left\{\left(\frac{\mu\varepsilon}{2}\right)\left[\left(1+\left(\frac{\sigma}{\omega\varepsilon}\right)^2\right)^{1/2}-1\right]\right\}^{-1/2} \qquad (3.2)$$

where ω is the angular frequency, ε, σ and μ are the permittivity (F/m), conductivity (S/m), and magnetic permeability of the materials respectively. In biological materials, μ in tissues has essentially the same value as that of free space, $4\pi \times 10^{-7}$ H/m.

The skin depths of tissues with low water content such as fat and bone are greater than those with higher water content such as muscle and skin. Table 3.1 contains typical skin depths for low and high water content tissues at selected frequencies.

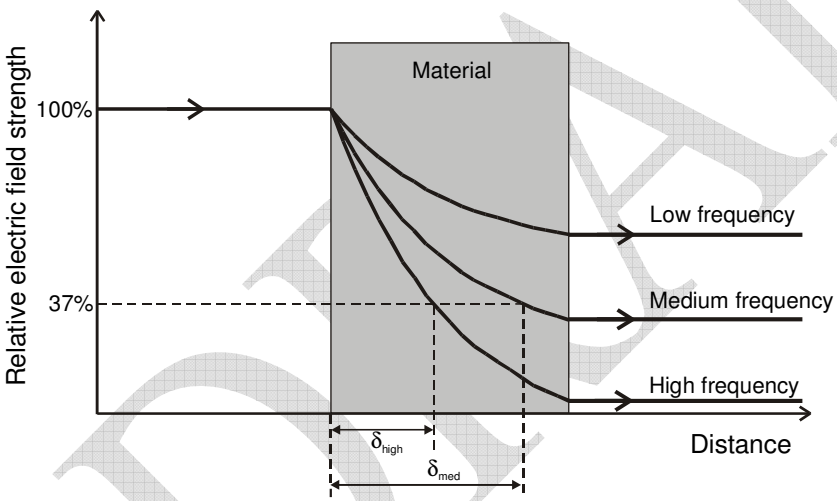

Figure 3.2. Illustration of how RF energy is absorbed in biological materials showing how the skin depth decreases with increasing frequency. Reflection of the incident radiation is assumed negligible at each interface in this diagram. The skin depth at high frequency, δ_{hi}, is less than that for medium frequency, δ_{med}.

Skin depth is also strongly frequency dependent. As is clear from Table 3.1 at around 150 MHz, bone and fat are poor conductors so they absorb energy weakly and the RF penetrates deeply into these tissues. High water content tissues such as muscle and skin on the other hand are good conductors and these will absorb more strongly and thus have a lower skin depth. At higher frequencies, the skin depth decreases, therefore absorption in the body becomes increasingly confined to surface tissues.

At mobile phone frequencies, of the order of 1 GHz or so, the skin depth in the brain is a few cm. Consequently most of the energy from the incident radiation is absorbed in one side of the head within a few centimetres of the handset. At 10 GHz the skin depth in most tissues is a few millimetres so almost all the energy

[2] For biological tissues in the radiofrequency range, this is generally a complex quantity, i.e. it has real and imaginary components that must both be taken into account.

will be absorbed in the skin and other surface tissues and there will be very little penetration into the deeper tissues of the body.

Table 3.1. The conductivity and skin depth of low and high water content tissues at selected radio frequencies*

	Tissues with low water content				Tissues with high water content			
	Fat		Bone		Muscle		Skin	
Frequency	Conduct -ivity (S/m)	Skin depth (mm)	Conduct -ivity (S/m)	Skin depth (mm)	Conduct -ivity (S/m)	Skin depth (mm)	Conduct -ivity (S/m)	Skin depth* (mm)
150 MHz	0.04	366.1	0.07	301.0	0.7	67.2	0.5	85.0
450 MHz	0.04	301.9	0.10	202.2	0.8	51.3	0.7	52.9
835 MHz	0.05	252.0	0.14	139.5	0.9	43.5	0.8	41.5
1.8 GHz	0.08	157.1	0.28	66.7	1.3	29.2	1.2	28.3
2.45 GHz	0.10	117.1	0.39	45.8	1.7	22.3	1.5	22.6
3 GHz	0.13	93.6	0.51	35.2	2.1	18.0	1.7	18.9
5 GHz	0.24	49.4	0.96	17.7	4.0	9.3	3.1	10.5
10 GHz	0.58	19.6	2.13	7.3	10.6	3.3	8.01	3.8

*The skin depth data in are calculated based on permittivity and conductivity of tissues taken from Gabriel et al. (1996b). The formula used for calculation of skin depth is taken from Griffiths (1989).

3.1.4.5 Type of tissue

The extent of reflection, absorption and transmission from an incident RF field depends on the type of material and its thickness in relation to the wavelength. When RF fields are incident on highly conducting (e.g. metal) surfaces, reflection is the dominant process; some absorption will occur and there will be almost no transmission. In the case of biological materials, there will be some reflection and the relative proportions of absorption and transmission will depend on the thickness of the material. Radio waves at telecommunications frequencies generally penetrate into the body tissues for a few centimetres before having been almost completely absorbed by the tissues (Table 3.1).

Absorption of energy also depends on the electrical properties of tissues which vary, mainly because some tissues are better electrical conductors than others. On exposure to RF fields, energy is not deposited uniformly throughout the body, even if the incident radiation has uniform power density. When radio waves are incident on a homogeneous slab of material, the proportion of energy transmitted decreases exponentially with the thickness of the slab. Consequently more energy will be absorbed in the material towards the front surface facing the incoming waves than towards the rear.

3.1.4.6 Heterogeneity of tissues

Biological systems such as the human body contain many different types of tissues that connect and interface with each other in many different conformations. Some tissues are extensively folded around each other, e.g. in the case of blood vessels within brain tissue, while others connect at smooth boundaries over large areas, e.g. the surfaces of bones. With such complex geometries, it is possible for internal focussing and reflection of RF fields to occur. Internal resonances can also occur where structures have comparable size to the wavelength. These processes lead to a very inhomogeneous distribution of absorbed RF energy even when the external fields to which the body is exposed are uniform. Only anatomically realistic computational models of the body are able to account for these physical processes and yield accurate predictions of absorbed energy at a detailed anatomical level. Such models are described later in this chapter.

3.2 Dosimetry

As explained above, the strength of the induced electric and magnetic fields inside the body are different from those outside. To assess the exposure of the body to an external EMF, one needs to determine

internal quantities (also called dosimetric quantities) which are related to the exposure in tissue (e.g. the induced electric field strength, induced current density and SAR). The process of determining internal quantities (dosimetric quantities) from external fields (exposure quantities) is called dosimetry. The role of dosimetry is to evaluate the induced quantities in the body and to correlate them with the biological effect of concern.

Chapter 4 of this document contains detailed discussions on different interaction mechanisms between RF EMF and the human body. The most recognised and well established mechanism for biological effects of RF radiation is tissue heating (Sheppard, Swicord & Balzano, 2008). Therefore, the current international guidelines for human exposure (ICNIRP, 1998; IEEE, 2005) continue to be based on classical heating mechanisms and the avoidance of adverse effects that occur in relation to temperature rises. The dosimetric quantity of most relevance at frequencies up to 10 GHz, i.e, where RF energy penetrates appreciably into the body tissues, is therefore the SAR, which describes the rate at which energy is absorbed in tissues per unit mass. At frequencies above 10 GHz, incident power density is the dosimetric quantity that is most relevant because penetration of RF energy into the body tissues is very small. As frequency reduces below 10 MHz, nerve and muscle stimulation effects due to induced currents in the body become increasingly relevant. Therefore current density and/or induced electric field strength are also used as dosimetric quantities at frequencies below 10 MHz (ICNIRP, 1998).

Presently used guidelines and standards recommend a set of *basic restriction* values in terms of SAR (ICNIRP, 1998; IEEE, 2005). However, since it is not possible to measure SAR directly, the guidelines also define *reference levels* that are used in practical assessment of compliance with the basic restrictions under a real exposure scenario. These have been conservatively derived from the basic restrictions with the objective that if the reference levels are not exceeded, the basic restrictions are also observed. Dosimetry plays an important role in the implementation of guidelines especially in the derivation of the reference levels. Dosimetry is also important when the exposure exceeds the reference levels. In this case it is necessary to examine whether the exposure actually exceeds the basic restriction or not by means of dosimetry.

Dosimetry plays an important role in scientific research to assess the exposure of people to RF EMF. The International EMF project of WHO emphasized the importance of well-defined exposure conditions for biological experiments in order to achieve meaningful interpretation and reproducibility of the result (Repacholi, 1998). Kuster and Schönborn (2000) published the minimum requirements of exposure systems for biological experiments addressing health effects of RF exposure.

There are different dosimetric methods available; experimental and numerical (theoretical) dosimetry techniques can be used to assess internal fields for different sources and geometries. Each method has advantages and disadvantages. For example, numerical dosimetry using realistic biological models can provide very fine spatial distribution of SAR and induced current density. However, actual exposure conditions from a real source can only be assumed in numerical dosimetry because the source has to be modelled. On the other hand, there are practical limits to the anatomical detail that can be incorporated into physical models and tissue boundaries would be disturbed if a measurement probe were manipulated inside them to measure the induced fields. Both methods are described in detail in the following sections. Usually, scientists, select one of the dosimetry techniques suitable for a particular exposure scenario, and validate the evaluated dose quantities by comparing results between numerical and experimental dosimetry.

3.2.1 Assessment of SAR

The SAR inside the body exposed to RF fields can be assessed by dosimetric tools; namely experimental and numerical techniques. Depending on the exposure scenario and the position of the RF field source with respect to the body, whole body SAR or localised SAR values can be obtained and compared with basic restriction values in the guidelines.

Significant temperature rise could occur if body parts are exposed to extremely localised exposures, leading in thermal injury of the tissue irrespective of the deep-body temperature elevation. In these situations, the local SAR in the part of the body is considered as the dosimetric quantity of interest. Temperature elevation in different body parts, however, is not necessarily proportional to the local SAR because of the heat conduction and transportation of heat by blood flow. Therefore, estimation of local temperature rise as an additional dosimetric quantity can also sometimes also be undertaken.

3.2.2 Mass-averaged SAR

Rise in deep (core) body temperature is related to the "average" energy absorption rate in the body, whereas temperature rise in organs, like the eyes and brain, depends primarily on the energy absorption in these organs (ICNIRP, 1998). Therefore, SAR is usually averaged either over the whole body mass, or over a small sample volume or mass of tissue, depending on the spatial pattern of the energy absorption in the body and where temperature rises are expected.

The averaging mass serves two purposes: firstly, it provides a definition of SAR that is robust and not overly sensitive to slight changes in exposure set-up; secondly, it takes into account the spatial dispersion of the deposited energy which is provided by heat transfer mechanisms (NRPB, 2004a). The SAR values are highly dependent on the geometry of the part of the body exposed and on the exact location and geometry of the source.

For frequencies up to a few GHz, as used in wireless communications, SAR is normally averaged over either 1 or 10 g. The averaging mass should be large enough to maximise the correlation with local temperature elevation (Hirata, Shirai & Fujiwara, 2008). It is suggested that an averaging mass of 10 g is a more appropriate parameter when the correlation between SAR averaging mass and the elevated temperature is investigated (Hirata, Shirai & Fujiwara, 2008; Razmadze et al., 2009).

The dominant factors influencing the correlation between mass-averaged SAR and temperature elevation are the thermal diffusion length[3] in the biological tissue, which largely depends on the blood perfusion rate, and the penetration depth of the RF waves (Hirata & Fujiwara, 2009).

One of the rationales for the 10 g averaging mass is based on the temperature elevation in the brain and eye lens, which has been computed with anatomically-based head models. The choice of averaging mass is clearly most important for highly localised exposure. At the other extreme, a uniform SAR distribution gives the same spatial average whatever mass is used. The greatest differences between 1 g and 10 g values are expected for situations of near-field exposure to a small antenna such as that of a mobile phone (NRPB, 2004a). Also, these averaging masses may not be appropriate for estimating temperature rises close to metallic medical implants where significantly higher SAR values are calculated when it is averaged over 1 g (Kyriakou et al., 2012; McIntosh, Iskra & Anderson, 2014).

3.3 Biological models

3.3.1 Physical and numerical phantoms

For health risk assessment, it is necessary to directly evaluate SAR, possibly from temperature rise, or to evaluate SAR from the induced electric field strength in a human body exposed to RF EMFs. However, it is very difficult to measure the internal electric field strength or temperature elevation in the human body using non-invasive methods. Therefore a surrogate of the human body, a so called "phantom" is used. A phantom designed to replicate the human body should exhibit similar interaction mechanisms with RF to those of a real human body. It can be a physical model, made from different organic and non-organic materials to replicate the electrical properties of various human tissues. It can also be a numerical model, which is an anatomically realistic computer model of typical people or animals, with values of the electrical properties for the different simulated tissues assigned to them. However, such phantoms generally do not include blood flow, which is an important heat transportation mechanism in living systems. For this reason, temperature rises derived in such phantoms will generally be higher than those produced in the body.

Physical phantoms are used in experimental dosimetry; the set-up usually consists of other components such as emulators that represent the base stations to which sources used near the body would normally connect with, implantable electric field sensors, a spatial scanning system, remote control and data recording systems. Alternatively, the distribution of induced electric field strength and the corresponding SAR values in the body can be estimated by solving Maxwell's equations utilising different mathematical methods such as finite difference time domain (FDTD) calculations (Tavlove & Hagness, 2005).

[3] Thermal diffusion length is the distance range from the point of maximum temperature elevation within which the majority of thermal energy transfer takes place. This is comparable to the concept of skin depth when electromagnetic waves are absorbed in a conductive medium, and is the distance at which the temperature elevation has reduced to 1/e (i.e. 63%) of its value at the point of maximum elevation.

3.3.2 Models of animal and human body

3.3.2.1 Experimental models

Phantoms for RF dosimetry are required to simulate the electrical properties equivalent to those of the human body. Various types of materials have been developed for phantoms and their references may be found in international standards on RF dosimetry (IEC, 2005; 2002).

Phantoms made from organic materials have been widely been used for RF dosimetry. Water and gelatine are amongst the main ingredients in phantom recipes as they are relatively easy to prepare and to adjust for their electrical properties. They are also suitable for SAR measurements where an electric field probe is inserted into the phantom for scanning. On the other hand, these materials have poor stability of their electrical properties due to water evaporation. Attempts have been made to make dry phantoms with high stability; however they require complex and skilled procedures and are costly (Kobayashi et al., 1993; Nikawa, Chino & Kikuchi, 1996).

Electrical properties are frequency-dependent and also vary according to the tissue's composition and structure such that homogenized tissues do not necessarily have the same electrical properties as those with cellular structures etc preserved intact. High-water-content tissues such as muscle are usually made with wet material whereas recipes for low-water-content tissues such as fat and bone are made with dry material.

Each phantom recipe can simulate the electrical properties of a tissue from several hundred MHz to several GHz (Hartsgrove, Kraszewski & Surowiec, 1987; Okano et al., 2000). It is however difficult to adjust the electrical properties of the phantom within small deviation, e.g. 5 %, from those of the actual biological tissues over broad frequency ranges. Different recipes optimized to the target electrical properties at each frequency are therefore used for critical measurements such as SAR compliance tests (IEC, 2005).

Several studies have attempted to develop broad-band phantoms (Gabriel, 2007; Lazebnik et al., 2005; Youngs et al., 2002). However, in adjusting both real part and imaginary part of the complex permittivity of the phantom to the target values simultaneously, the uncertainty of the electrical properties measured by commercially available systems, temperature change and water evaporation are amongst the difficulties that need detailed consideration (Fukunaga, Watanabe & Yamanaka, 2004).

It is also very difficult to develop a heterogeneous structure using organic materials such as water and gelatine. Moreover, the boundaries in such structures would be disturbed if a measurement probe were manipulated through them or in their vicinity. Therefore, homogeneous tissue is generally used as a liquid inside shaped hollow shells in order to form physical phantoms. For instance, a standardised phantom in the shape of a hollow head is usually used for compliance tests of cellular phones (IEC, 2005; IEEE, 2003). A full-size model of the human body was first developed by Olsen (1979) and by Olsen and Giner (1989). Stuchly et al. (1987) developed a whole-body phantom which simulates heterogeneous structure with solid material for bone within a liquid phantom for high-water content tissues such as muscle. They measured electric field distributions by scanning with a field probe inside the heterogeneous phantom. Several heterogeneous head phantoms have also been developed for SAR evaluation during use of a mobile wireless handset (Cleveland & Athey, 1989; Okano et al., 2000).

3.3.2.2 Numerical models

Simple models such as spheres and ellipsoids are amenable to analytical solutions and can be used to characterize the RF energy absorption in a human body. Durney et al. (1986) systematically reviewed and summarized these models and their use in research leading to the development of early RF safety guidelines.

Over the past 20 years, dosimetric techniques have been transformed by the use of voxel-based anatomical human-body models and the application of computational methods for the calculation of internal electromagnetic quantities. A voxel (volume pixel) represents a small volume element (or cube) of a tissue with dimensions as small as a few millimetres on each side. Thus, a whole-body human voxel model can consist of many million voxels. The computational algorithms are usually based on the Finite Difference Time Domain (FDTD) method, with some researchers writing their own codes and others using commercially available codes.

Several laboratories have developed whole-body animal and human voxel models (Dawson, Caputa & Stuchly, 1997; Dimbylow, 2005a; b; Dimbylow, 1997; Furse & Gandhi, 1998; Lee et al., 2006; Mason et al.,

2000b; Nagaoka et al., 2004). The most widely used voxel model in RF dosimetry was developed by the Brooks AFB Laboratory and based on the database of the Visible Human Project (VHP). Mason et al. (2000a) investigated the effect of different dosimetric parameters on the characteristics of absorption in the VHP Man.

Other whole body human voxel models have been developed that are more representative of the average height and weight values of people, as specified by the International Commission on Radiological Protection (ICRP, 2002) and other organisations. Female phantoms have also been developed, e.g. by Dimbylow (2005b) and by Nagaoka et al. (2004).

Dosimetry studies have now become more advanced and inclusive, with the development of whole-body human voxel models in different postures, as well as those of children, and pregnant women containing foetuses and embryos. Some of these models were developed by deforming standing adult human models (Cech, Leitgeb & Pediaditis, 2007; Dimbylow, 2006; Findlay & Dimbylow, 2005; Kainz et al., 2003; Nagaoka et al., 2007; Wang et al., 2006). However, whole-body child models have now been developed based on datasets from actual children (Christ et al., 2010b; Lee et al., 2006).

Realistic numerical models are developed from images taken by MRI or CT scans. MRI images have generally better quality than those obtained from CT scans, and are useful in identifying interior tissues because high contrast images of different soft tissues can be formed. In order to develop a voxel model for FDTD calculation, original gray-scale images from the scans are interpreted into tissue types, referred to as segmentation. Since the gray scales in MR images do not correspond to tissue types directly, the tissue and organ identification processing has to be performed manually to a large extent. Even if software for automatic identification is applied, manual verification or correction is required. Recent models of the whole human body have up to about 50 tissue types, and the finest resolution is about 1 mm.

Intrinsic limitations of voxel-based models are that they do not contain any spatial information at scales smaller than their native resolution and that they cannot be easily deformed to adopt different postures. These problems can be overcome by adopting a computer aided design (CAD) approach to develop models in which the organ and tissue boundaries are represented by parametric surfaces. Christ et al. (2010b) developed a CAD-based human model which can easily move and rotate in any direction with 3-D CAD software and no limitation of their spatial resolution. The surfaces of the model can be readily deformed, but care must be taken for the joints of the body to be correctly articulated. CAD models are usually segmented into voxel models at the required resolution before carrying out FDTD calculations.

It is notable that, although many sophisticated and complex numerical models have been developed in recent years, most results of the realistic voxel models have generally agreed with those of the simple anatomical models of the whole body in terms of the whole-body SAR that results from a given plane-wave exposure condition.

3.3.3 Dielectric properties of tissues

Biological tissues contain free and bound charges, including ions, polar molecules and an internal cellular structure. When an external electric field is applied to tissues, the electric charges are shifted from their original position, causing polarisation and ionic drift, and the establishment of displacement and conduction currents. Dielectric properties of tissues (permittivity and conductivity) are measures of these effects which determine the interaction of electric fields with human body. The availability of dielectric data for different tissues is therefore vital for both experimental and computational dosimetry techniques.

Dielectric properties of tissues are frequency-dependent and arise as a consequence of particular mechanisms of polarisation, each of which has a maximum frequency at which it can occur. The effect of each mechanism is to cause a "dispersion" in the frequency spectrum of the tissues electrical parameters (the dielectric spectrum). Biological tissues are affected by three main dispersions predicted by known interaction mechanisms. At low frequencies the α dispersion is associated with ionic diffusion processes at the site of the cellular membrane. At intermediate frequencies (kHz region), the polarisation of the cellular membrane, which is a barrier to the flow of ions between the intra and extra cellular media, is the main cause of the β dispersion. Finally, the γ dispersion around the GHz frequency regions mainly due to the polarisation of water molecules inside the tissues. Dielectric properties of tissues vary according to the physiological state of the tissue, the intactness of the cellular membrane and the water content. The α and β dispersions would have importance in the present RF context only if demodulated low frequency signals could arise in tissues through a non-linear

mechanism, and if these low frequency signals were strong enough to act through a mechanism with a biological outcome (see Chapter 4).

Several techniques exist to assess the dielectric properties of biological tissues. One widely used procedure involves the use of coaxial contact probes and measurement of the reflection coefficient followed by numerical deduction of the dielectric properties of the sample based on a theoretical model of the impedance of the probe (Gabriel, 2000).

The early literature on the dielectric properties of body tissues has been reviewed by Gabriel et al. (Gabriel, Gabriel & Corthout, 1996) who also produced their own data (Gabriel, Lau & Gabriel, 1996a) and developed parametric models to reproduce the relative permittivity and conductivity as a function of frequency (Gabriel, Lau & Gabriel, 1996b). This database has been used extensively in dosimetry studies since it was created. Recently, new dielectric data have been collected from live porcine tissues, which are thought to be a good animal-based substitute for human tissue. This also provides an added dimension to the comparison with the data from the 1996 database that were mostly derived from measurement on excised ovine tissue (Gabriel, 2005; Peyman et al., 2007).

Until recently, the literature data consisted mostly of dielectric properties of tissues from mature animals with a few older studies reporting systematic changes in the dielectric properties of ageing brain tissues (Thurai et al., 1984; 1985). More recent studies looked at the variation of dielectric properties of several rodent, porcine and bovine tissues as a function of animal age and found similar trends (Gabriel, 2005; Peyman, Rezazadeh & Gabriel, 2001; Peyman et al., 2007; Peyman et al., 2009; Schmid & Überbacher, 2005). The results of these studies generally showed a significant decline with age in both permittivity and conductivity of tissues with high water content such as long bone, skull, skin, muscle and bone marrow. At around the GHz frequency region, the observed variations are mainly due to the reduction in water content of tissues as animals age. In the case of brain, increased myelination and decreased water content as a function of age is suggested to be the reason for the drop in permittivity and conductivity values of white matter and spinal cord as animals age, as observed by Schmid and Überbacher (2005) and Peyman et al. (2007). The largest variation in the dielectric properties as a function of age is observed in bone marrow tissues due to the transformation of high water content red marrow to high fat content yellow marrow as the animal grows (Peyman et al., 2009).

These studies raised a question over the extent to which the variation of dielectric data as a function of age may affect the results of dosimetry in animal exposure studies, and consequently, the possible implications for studies assessing the exposure of children. The dielectric spectra of ageing porcine tissues have been parameterized to allow their use at any frequency or multiple frequencies within the confines of the models of children (Peyman & Gabriel, 2010).

3.4 Parameters affecting SAR

The effect on SAR of frequency, dielectric parameters, voxel size, polarisation of the incident electric field, shape and size of the model, and posture is reported in several papers, for example, Mason et al. (2000a); Findlay and Dimbylow (2005) and Uusitupa et al. (2010), and have been mentioned in Section 3.1.4.1.

Until recently, the majority of dosimetric studies were focused on models of human adults. However, increasing use of telecommunication devices amongst the young has led to research into the differences in the exposure of children and adults.

The two main factors differentially affecting the exposure of children and adults are changes in the physical size of the body and in the dielectric properties of tissues (see above). The earlier dosimetric studies used adult human models and scaled them down linearly to approximate a child of a given height and mass while using the dielectric properties of adult tissues (Gandhi, Lazzi & Furse, 1996; Gandhi & Kang, 2002; Wang & Fujiwara, 2003). Later studies developed children's head models from magnetic resonance images of children to obtain a more realistic assessment of the exposure of children (Anderson, 2003; Christ & Kuster, 2005; Dimbylow & Bolch, 2007; Lee et al., 2009; Schönborn, Burkhardt & Kuster, 1998).

In considering the dosimetry results from models that use linearly scaled adults to represent children, it is important to recognise that the dimensions of different body structures grow at different rates during the course of development. For example, children have proportionately larger heads than adults. Thus, overall body morphology changes with age, and dosimetry results from scaled adult models should not generally be considered reliable for children, irrespective of dielectric considerations.

3.4.1 Whole body and localised SAR

As explained above, the thermal effect is the dominant established biophysical mechanism in leading to biological and health effects of RF exposures, and the current guidelines on limiting human exposure are based on limiting heating. Elevation of deep body temperature is closely related to the energy absorption rate in the whole body, or whole-body average SAR (ICNIRP, 1998). Thus dosimetry of RF exposure is generally equivalent to the determination of SAR in the body exposed to RF fields.

In the case of extremely localised exposures on some body part, a biologically significant temperature rise could occur around the exposed part resulting in thermal injury of the tissue regardless of the deep-body temperature elevation. Local SAR in the part of the body should be considered in this case. Temperature elevation in the body part, however, is not necessarily proportional to the local SAR because of the heat conduction. Thus dosimetry of RF exposure sometimes includes measurement or estimation of temperature as an adjunctive dose metric since it is more directly related to thermal injury.

3.4.2 Age and size related variations

The effect of age on the calculated SAR could be due to the difference in dielectric properties of younger and older tissues as well as changes in the size and shape of the body/head.

3.4.2.1 Variation in dielectric properties

Some studies have used measured dielectric properties of tissues as a function of age to calculate SAR values in models of children's head/body as a result of exposure to EMFs (Christ et al., 2010a; Gabriel, 2005; Peyman et al., 2009). A few other studies have used adult dielectric properties and adjusted them for younger tissues, assuming higher water content (Dimbylow, Bolch & Lee, 2010; Keshvari, Keshvari & Lang, 2006; Wang et al., 2006). Each of the following three studies have used a different metric in their SAR calculation, such as localised SAR_{10g} values for individual tissues, SAR averaged over 10 g of tissues in the shape of a cube and whole body SAR, therefore a direct comparison cannot be drawn.

Gabriel (2005) used age-related dielectric properties of rat tissues in a numerical study of exposure of rat models to plane waves at 27, 160, 400, 900, and 2000 MHz. A total of 34 tissue types have been examined in three rat models (10, 30 and 70 days old), from which only 9 tissues exhibited variation in their dielectric properties as a function of age. The results showed that, although changing the tissue dielectric properties would affect the localised SAR, no clear pattern could be established. The effect on whole body SAR was reported to be small, its extent depending on the variation in properties and the abundance of the tissues in the exposed model. These results can be explained as due to the fact that changes in dielectric properties would affect the coupling with the body and the interaction of tissues with the EMFs. It is also important to isolate the effect of changing tissue properties from all other factors that would affect the exposure, such as the size of the animal, and polarization and direction of the incident field (Gabriel, 2005).

The second study examined the sensitivity of calculated SAR averaged over a 10 g cube in one adult and two child head models exposed to EMF from walkie-talkie devices operating at 446 MHz (Peyman et al., 2009). Head models representing adults and 3- and 7-year old children were considered with tissue dielectric properties taken from 10 kg , 50 kg and 250 kg pigs, which were taken as representative of children in the range 1-4 years old, children in the range 11–13 years old and adults respectively. The results showed that variations in SAR_{10g} were less than 10% for the investigated configuration and that the variations of the tissue properties are not clearly reflected as a variation in SAR_{10g} . This could be because spatial averaging of the SAR dilutes the effect of changes occurring in masses smaller than 10 g. In addition, different head tissues do not contribute equally in the cubical averaging volume and not all tissues in the averaging volume have the same variation of the dielectric properties with age (in this case only skin contributed to the variation within the 10 g cube).

Finally, Christ et al. (2010a) studied the exposure of three anatomical head models (adult, 3- and 7-year old) to a generic dual band mobile phone operating at 900 MHz and 1800 MHz. They incorporated 16 tissue types in the models by assigning dielectric properties of 10 kg, 50 kg and 250 kg pigs. Although the results showed SAR variations due to the age-dependent changes to be within 30%, for all the configurations analysed, age dependencies of dielectric tissue properties did not lead to systematic changes of the 10 g peak spatial SAR. In other words, the hypothesis that variation in the dielectric parameters results in larger exposure of young mobile phone users could not be confirmed. The authors suggested that this may be due to the fact that highest

519 age-dependent variations occur in tissues with low water content, where the SAR would be lower than in the
520 higher water content tissues.

521 The dielectric properties of bone marrow exhibit the largest variation with animal age, as reported by
522 Peyman et al. (2009). As the distribution of bone marrow in the skull is very complex, Christ et al. (2010a)
523 examined the impact of age dependent changes of dielectric properties with the help of a generic planar layered
524 model consisting of skin, fat, bone, marrow, bone again and then muscle. The authors calculated the 10 g peak
525 spatial SAR averaged over bone marrow tissue. The absorption in the bone marrow was largely independent of
526 the layer thickness and clearly age dependent. The results showed that exposure of the bone marrow of children
527 might exceed that of adults by about a factor of ten. This is due to the strong decrease in electric conductivity of
528 this tissue with age. These results are yet to be confirmed in anatomically realistic models exposed to realistic
529 sources.

530 *3.4.2.2 Variation in shape and size of head*

531 When a small transmitter like a mobile phone is held to the head, there are various general
532 considerations that relate to the distribution of SAR that results in the head. The SAR distribution will be
533 maximal in proximity to the radiating part of the transmitter and will generally reduce through the head as
534 distance increases. Thus, the SAR averaged over the entire head (or brain) will be higher for smaller heads than
535 with larger heads exposed under the same conditions. The radius of curvature of the head in the vicinity of the
536 transmitter is important because a small radius of curvature, as with the child's head, will mean less of the head
537 tissue will be in the immediate proximity of the transmitter and tend to produce lower averaged SAR in the head
538 as a whole. However, the ear acts as a spacer, increasing distance of the transmitter from the head and therefore
539 reducing averaged SAR in the head. Thus, a thinner and more compressible ear, as with a child, will result in
540 higher averaged SAR in the head.

541 The size of the radiating part of a transmitter (antenna) is also a factor affecting the SAR distribution
542 in the head because a larger source will produce a more diffuse input of RF energy to the head tissues than will a
543 smaller source. Overall, antennas reduce in size with increasing frequency and mobile phones have also reduced
544 in size as the technology has developed. Both of these considerations could lead to hypotheses about how
545 localised SAR averaged over 1 g or 10 g might vary with frequency and how they might have changed over time.
546 However, in terms of age-related variations, the situation is complicated, with various factors that can trade-off
547 against each other such that it is difficult to determine without investigation whether localised 1 g or 10 g SAR in
548 the head from a mobile phone would typically be greater or smaller in a child's head than in that of an adult.

549 Gandhi et al. (1996) were amongst the first to use a linearly-scaled child head model with adult
550 dielectric properties to compare the exposure of adults and children to mobile phones. They found a deeper
551 penetration and increase of 50% in the maximum 1 g averaged SAR in the child's head.

552 Hombach et al. (1996) examined the energy absorption in a human head at 900 MHz, and reported
553 that the spatial peak SAR is affected by the size and the shape of human head at a defined distance from source.
554 On the other hand, the authors reported that the effects caused by the complex anatomy are minor in the case of
555 volume-averaged values because these do not exceed the results found in a homogeneous head model.

556 Schönborn et al. (1998) used a scaled adult model and two realistic child head models using MRI data
557 for similar comparisons, but did not report any significant differences between the exposure in adults and
558 children. Bit-Babik et al. (2005)(reported that the peak local average SAR over 1 g and 10 g of tissue and the
559 electromagnetic penetration depths are about the same in head models of adults and children under the same
560 exposure condition.

561 De Salles et al. (2006) reported that under similar exposure conditions (850 and 1850 MHz), the 1 g
562 SAR calculated for children is higher than that of adults. The authors claimed that when using a 10-year old
563 child model, SAR values are 60% higher than those obtained for adults.

564 Attempts to repeat the above studies by other researchers have produced contradictory results, in
565 particular when different normalisations were performed for output power or antenna current. In addition,
566 differences in averaging procedures used to determine spatial peak SAR meant there was a need for further
567 studies using a standardised approach (Bit-Babik et al., 2005; Wang & Fujiwara, 2003). Some of the subsequent
568 studies reported a higher SAR in the head models of children (Anderson, 2003; Wiart et al., 2008) while others
569 did not find any significant difference in SAR between adult and child models or could not reach a conclusion

(Christ & Kuster, 2005; Fujimoto et al., 2006; Keshvari & Lang, 2005; Lee, Choi & Choi, 2007; Martínez-Búrdalo et al., 2004; Wang et al., 2006).

In 2006, a large study was carried out involving 14 laboratories to study the differences in SAR for adults and children who are exposed to mobile phones (Beard et al., 2006). A single protocol was followed by all the participants using the Specific Anthropomorphic Mannequin (SAM) homogeneous head model designed for mobile phone compliance measurements, an anatomically realistic adult head model and a scaled 7-year old child head model. Two operating frequencies of 835 and 1900 MHz and two phone positions, denoted cheek and tilt, were considered. In addition, the SAR values were normalised to both the antenna input power and the feed point current. The results revealed a reverse effect at 1900 MHz, where the peak 1 g SAR values in the head of the adult model were higher in both head positions and for both normalisation scenarios. At 835 MHz however, the SARs were higher in the child model than the adult model in particular in the tilt position and when normalizing to antenna current.

Hadjem et al. (2005) found that brain exposure depends on the morphology of the ear and Wiart et al. (2008) reported higher exposure of the cerebral cortex in children than in adults.

In summary, the overall evidence from studies on the exposure of children's heads does not draw a consistent picture to support the assumption that the SAR level in a child's head is higher than that for adults. This arises because the results are highly model-specific and power absorption in the head is influenced by many factors. It is also notable that even the higher SAR values reported in some of the studies for children's heads, are below the 2 W/kg ICNIRP basic restriction.

3.4.2.3 Variation in shape and size of body

The effects of body size in relation to the wavelength have been discussed in general terms earlier in this chapter, and pertinent studies are reviewed here. As with the studies above regarding the head, the differences between the exposure of children and adults are an important theme in the literature.

It is established that the whole body SAR depends on the size of the body, and this has been considered when the ICNIRP reference levels were set. Starting from the premise that an SAR of 4 W/kg for a healthy adult is equivalent to a 1°C temperature rise, there is a 50-fold reduction in deriving the basic restriction on whole body SAR for the general public (0.08 W/kg). In principle, this reduction factor should be sufficient to take into account all the variations due to different dosimetric factors, including body size. However, it is now apparent that the basic restriction on exposure for small children under worst case exposure conditions may be slightly exceeded at the public reference level (NRPB, 2004a; 2004b). This is supported by studies carried out for phantoms modelling children in the age range from 9 months to 11 years, which found that whole body SAR restrictions are exceeded in two frequency ranges: 45–170 MHz and 1400–4000 MHz (Bernardi et al., 2003; Dimbylow & Bolch, 2007; Dimbylow, 1997; 2002; Mason et al., 2000a; Tinniswood, Furse & Gandhi, 1998; Wang et al., 2006). Dimbylow (2007)) reported that, when using a phantom of a 9-month old baby at a frequency of 1.6 GHz, the whole body SAR was equal to the basic restriction when the electric field strength was 0.83 times the value of the reference level. Thus, exposure at the reference level would result in the whole body SAR restriction being exceeded by about 40%, given that SAR is proportional to the electric field strength squared . Higher SAR levels were also observed in phantoms modelling children aged 3, 5, and 7 years in the frequency region around 2 GHz (Conil et al., 2008; Hirata, Asano & Fujiwara, 2007; Neubauer et al., 2009). Figure 3.3 shows a typical set of results illustrating that the reference level is not conservative over the basic restriction in certain frequency ranges with smaller body sizes.

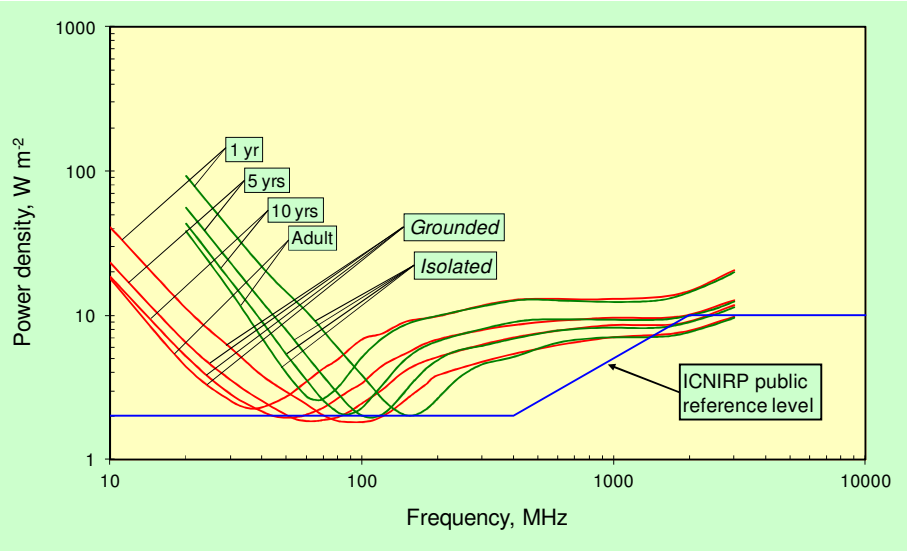

611

612 **Figure 3.3.** Curves showing the power density of a vertically polarized plane wave incident on the front of the
613 body required to produce a whole-body SAR equal to the basic restriction with different size phantoms and
614 different grounding conditions (Dimbylow, 2005a; 1997).

615 The polarization of the incident wave can also affect the calculated SAR, as studied by Hirata and
616 Fujiwara (2009) on whole body averaged SAR in an infant model. The authors reported that whole body
617 averaged SAR for plane-wave exposure with vertically aligned electric field is smaller than that with a
618 horizontally aligned field for frequencies above 2 GHz. This could be due to the component of the surface area
619 perpendicular to the electric field of the incident wave (Hirata & Fujiwara, 2009).

620 Uusitupa et al. (2010) also suggested that the effect of polarization must not be neglected. They
621 reported that near the whole-body resonance, polarization has a strong effect on whole body SAR. They also
622 indicated that in the GHz region the effect may be more than 2 dB (i.e. a variation of 60%). Note, between 2 and
623 5 GHz for adults, whole body SAR is higher for horizontally polarised fields than for vertically polarized ones if
624 the incoming direction is in the azimuth plane. For a child, however, the effect of incoming direction is similar to
625 that of an adult, except at 300 MHz for horizontal polarization. Generally, it is suggested that in the GHz range
626 horizontal polarization gives higher whole body SAR than with vertically aligned fields (Kühn et al., 2009;
627 Vermeeren et al., 2008).

628 In summary, most of the studies conducted on whole body SAR, reported higher exposure for child
629 models than for adults in two frequency regions (around 100 MHz and 1–4 GHz). They also show that, within
630 these specific frequency ranges, an exposure to an electric field strength or plane wave equivalent power density
631 equal to the reference level can lead to whole body SAR exceeding the basic restriction by up to 40% under
632 worst case conditions. Thus, for children or small persons (shorter than 1.3 m) the reference levels of the
633 ICNIRP recommendations may not be conservative estimates. A review by ICNIRP (2009) acknowledges the
634 outcome of the above studies and concludes that this increase in SAR is negligible compared with the large
635 reduction factor of 50 applied in deriving the whole-body basic restriction for the general public (a reduction
636 factor of around 30 still remains). Similar conclusions were reached in comprehensive reviews carried out by
637 national authorities such as the Health Council of the Netherlands (HCN, 2011).

638 *3.4.2.4 SAR in the fetus*

639 Dimbylow (2007) reported that the whole body SAR is lower in pregnant women compared with non-
640 pregnant women and that the difference increases with gestation period. This is because the whole body
641 averaged SAR depends inversely on the mass, which increases during pregnancy while the height remains
642 constant. The study also found that the fetus's maximum whole body SAR occurs at 70 MHz for conditions
643 where the mother is isolated from ground and SAR levels in the fetus are lower compared with those in the
644 mother. The results also confirmed that the ICNIRP reference levels are sufficient to guarantee compliance with
645 the basic restriction for plane wave exposure. Two more studies reported similar results and confirmed
646 compliance with ICNIRP guidelines (Nagaoka et al., 2007; Togashi et al., 2008). Kawai et al. (2006) developed
647 a model of the abdomen of a pregnant woman based on MR images of Japanese women in late pregnancy period.

They then assessed the local 10 g averaged SAR of a foetus inside this abdomen to be less than 1.5 W/kg when exposed to 150 MHz signals with the maximum power of 5 W used for portable radio terminals in Japan. The same authors (Kawai et al., 2010) reported the maximum average SAR in the embryos exposed to plane waves to be lower than 0.08 W/kg when the incident power density is equal to the ICNIRP public reference level.

3.4.3 Posture and grounding effects

A change in the posture of the human body can significantly affect the way in which it absorbs RF EMFs. Findlay and Dimbylow (2005) studied the effects of posture on FDTD calculations of specific absorption rate in an anatomically realistic model of the body which was modified to develop new voxel models in postures other than the most commonly analysed standing position with arms to the side. The scenarios considered were sitting, arms stretched out horizontally to the sides and arms raised vertically above the head. The results showed that the effect of a raised arms posture lowered the resonant frequency and increased the value of the whole-body averaged SAR at resonance by up to 35% when compared to the reference arms by the side position. They also reported that in certain postures external electric field reference levels alone would not provide a conservative estimate of localised SAR exposure and it would be necessary to invoke secondary reference levels on limb currents to ensure compliance with ICNIRP's basic restrictions. A similar study was carried out for SAR in a 7-year old child voxel model (Findlay, Lee & Dimbylow, 2009). It reported that raising the arms increased the SAR by 25%.

Uusitupa et al. (Uusitupa et al., 2010) suggested that body posture has little effect on whole-body SAR in the GHz region, but at around 300-450 MHz, one may even expect a 2 dB rise (+60%) in whole-body SAR if posture is changed from the default standing position to a sitting position. The authors also concluded that posture affects peak 10 g SAR (in head and trunk and limbs) much more than whole-body SAR.

3.5 Temperature elevation

Temperature elevation can be considered as the main factor able to cause adverse health effects in the human body when it is exposed to external RF EMF. It results from energy deposited or absorbed in body tissues through local, partial-body or whole-body exposures.

The extent of tissue temperature rise depends on several factors including the pattern of energy absorption, the pathways through which heat is transferred and removed from the tissues inside the body, heat exchange between the body surface (skin) and the external environment, and the thermoregulatory process.

It is impossible to non-invasively measure the temperature rise inside the body; however computational simulations based on the internal distribution of SAR can be used to make estimations.

Pennes (1948) proposed the so called "bioheat" equation to calculate the time variation of temperatures in a human body. It gives the temperature distribution, $T(r,t)$, which is a function of location and time inside the body taking into account the SAR distribution, $Q_v(r)$, expressed as SAR divided by the volume density $\rho(r)$.

$$\nabla \cdot (K(r)\nabla T) + A(r,T) + Q_v(r) - RL(r) - B(r,T)(T - T_B) = C(r)\rho(r)\frac{\partial T}{\partial t} \quad [\mathrm{W/m^3}] \qquad (3.3)$$

The bioheat equation takes into account several factors such as the tissue thermal conductivity, K (W/m °C), metabolic heat production A (W/m^3), respiratory heat losses from lungs RL (W/m^3), difference between blood and tissue temperature ($T-T_B$) and the heat exchange due to capillary blood perfusion B (W/°C per m^3), which is proportional to blood flow.

Originally, the bioheat equation did not account for thermoregulatory response, and thermal responses were later considered by using very simplified models of human bodies (Stolwijk & Hardy, 1977). Foster and Adair (2004) tested the response of the model by using experimental data from human volunteers. Finally, Bernardi et al. (2003) incorporated the thermal response model within the bioheat equation; which can be used to estimate the temperature elevation in an anatomically-based human body model in the time domain.

Although the bioheat equation estimates the temperature distribution in the body as a function of time, for pulsed or brief applications of RF energy, the exposure duration is not long enough for significant conductive

or convective heat transfer to affect tissue temperature rise. In this case, the initial rate of rise in temperature is related to SAR as follows:

$$\Delta T = \frac{SAR}{C}\Delta t \qquad (3.4)$$

where ΔT is the temperature increment (°C), C is the specific heat capacity of tissue (J/kg[1] °C), and Δt is the duration of RF exposure. Equation (3.4) shows that the rise in tissue temperature during the initial transient period of RF energy absorption is linearly proportional to SAR and inversely proportional to the specific heat capacity of tissue.

Clearly, if the intensity and duration of the exposure are excessive, the RF energy can produce temperature rises that can result in adverse health effects due to heat stress or local tissue damage.

Under moderate conditions, a temperature rise on the order of 1°C in humans and laboratory animals can result from an SAR input of approximately 4 W/kg. However, such temperature rise falls within the normal range of human thermoregulatory capacity. Above this temperature or SAR value, disruption of work in trained rodents and primates has been reported for normal environmental conditions (ICNIRP, 1998).

3.5.1 Localised exposure and thermal time constants

In estimating the localised temperature elevation in the human body as a result of localised exposure, one needs to consider the balance between the rate of RF power deposition and the time constants for heat convection by blood flow and heat conduction. For sufficiently high whole-body and intense-localised exposure, the absorbed EM energy becomes appreciable in comparison with basal metabolism (around 1 to 2 W/kg typically) and leads to body-core temperature elevation (Adair, Mylacraine & Allen, 2003; Guy et al., 1975). A proportion of the RF energy absorbed locally is transferred as heat to the body core via blood flow, which leads to the activation of centrally mediated (e.g. through sensors in the brain) thermoregulatory responses in order to maintain core body temperature (Adair & Black, 2003).

The time taken for blood to be travel from a site of localised exposure to where its temperature is sensed centrally means that the thermal time constant of the body core is slightly longer than that associated with temperature elevation in a body part due to localised exposure. Moreover, thermal sensors are also located in the skin, which means that an adaptive thermoregulatory response often begins before an increase in core temperature. This is particularly the case when RF energy absorption is mostly confined to the surface of the body, as occurs with exposures towards the higher RF frequencies.

In addition, certain tissues, e.g. the brain, have higher rates of blood flow than other tissues, even when body core temperature is not significantly increased, and this mechanism can play an important role in limiting temperature rises for intense localised exposure (Wainwright, 2003).

3.5.2 Whole body exposure and thermal time constants

When estimating the whole body temperature elevation, it is important to take into account the variation in blood temperature. Bernardi et al. (2003) incorporated the blood temperature factor into the original bioheat equation. For example in the case of a plane-wave exposure at 40 MHz with a power density of 2 W/m^2 (equal to the ICNIRP reference level) the maximum temperature rise at the ankle is about 0.7 °C.

As mentioned before, the body's thermoregulatory response reduces temperature rise, particularly in the body core. Hirata et al. (2007) considered the far-field (plane wave) exposures of the naked body at two frequencies, 65 MHz (whole body resonance frequency) and 2 GHz, taking into account the effect of perspiration on body-core temperature elevation. The variability of temperature elevation caused by sweating was found to be 30%. A whole-body average SAR of 4.5 W/kg was required for a body-core temperature elevation of 1°C after 60 min exposure in the model of human with the lower sweating coefficient, while 8 W/kg was required with the highest sweating coefficients. The thermal time constant in the body core was 20 min and almost the same for both frequencies.

3.5.3 Temperature rise in the eye

Excessive temperature rise in the eyes is associated with several effects, including cataract formation. Guy et al (1975) reported microwave-induced cataract formation in rabbit eyes. Emery et al. (1975) developed a heat transfer model for the rabbit eye by assuming that the eye is an object thermally isolated from the rest of the head. Later works used anatomically based human models and improved heat transfer coefficients between the eye, the air and the rest of the head to quantify the temperature rise in the eye (Lagendijk, 1982).

Two studies reported a maximum temperature rise of 0.04–0.06 °C on the surface of the eye and in the lens when they are exposed to an incident power density of 10 W/m^2. The first study considered the frequency range 0.6–6 GHz (Hirata, Matsuyama & Shiozawa, 2000) and the second considered 6–30 GHz (Bernardi et al., 1998). These studies also confirmed that the maximum temperature elevation in the lens decreases with increasing frequency.

Several other authors who used improved heat transfer models and took into account the blood flow in the choroidal and retinal tissues as well as the heat transfer in the whole head reported a temperature rise of 0.3°C for an eye-average SAR of 2 W/kg (Buccella, De Santis & Feliziani, 2007; Hirata, 2005; Wainwright, 2007). As expected, a correlation was observed between the average eye SAR and the maximum temperature elevation in the lens. However, a lower temperature elevation was reported in Flyckt et al. (2007) using a heat transfer model involving discrete vasculatures (DIVA). Van Leeuwen et al. (1999) also used DIVA modelling and reported lower local temperature elevation around the blood vessel due to the cooling effect of blood flow.

3.5.4 Temperature rise in the head

Following increasing use of telecommunication devices, a considerable number of studies have been carried out on the temperature elevation in the head exposed to mobile phone handset antennas (Bernardi et al., 2000; 2001; Gandhi, Li & Kang, 2001; Hirata, Morita & Shiozawa, 2003; Hirata & Shiozawa, 2003; Hirata et al., 2006; Ibrahim et al., 2005; van Leeuwen et al., 1999; Wainwright, 2000; Wang & Fujiwara, 1999). Although some common assumptions were made, each of the above studies used a different type of antenna, head model and SAR metric, therefore a direct comparison between the results is not possible. The output power of a typical handset antenna is up to a few hundred milliwatts, which is much lower than the basal metabolic rate of an adult male of 100 W or more; therefore the above studies have all assumed a constant temperature for blood. Wainwright (2000) used a finite element thermal model to allow better simulation of the surface curvatures of the human head to calculate SAR and temperature elevation. Hirata and Shiozawa (2003) studied the correlation between peak spatial-average SAR and maximum temperature elevations in the head for different frequencies, polarizations, feeding positions, and antennas. The authors found fairly good correlations between peak spatial-average SAR and maximum temperature elevation in the head excluding the pinna. Hirata et al. (2006) investigated the correlation of maximum temperature rise in the head with peak SAR calculated by different average schemes and masses. For an exposure scenario involving a peak SAR of 10 W/kg (for 10 g of contiguous tissue and for exposure times of 60 min or longer), including and excluding the pinna, resulted in a maximum temperature rise of 2.4 or 1.4 °C in the head respectively. The authors also noted that a high degree of spatial correlation between peak SAR and maximum steady state temperature rise for durations of 60 min or longer is not expected, especially for exposures of large biological bodies with efficient thermal transfer characteristics (Hirata et al., 2006).

Other authors reported a temperature rise of about 2 °C in a head without pinna when peak SAR was 10 W/kg averaged over a 10 g cubic volume, which was higher than that for contiguous tissue volumes (Bernardi et al., 2000; Hirata & Shiozawa, 2003; Hirata, Shirai & Fujiwara, 2008; Razmadze et al., 2009; Wainwright, 2000).

The mobile phone handset (and its battery) placed close to the head can also behave as a source of conducted heat and reducer of convection from the skin surface, thereby causing local temperature rise (Bernardi et al., 2001; Gandhi, Li & Kang, 2001; Ibrahim et al., 2005). The skin temperature elevations due to these processes have been shown to be 1°C or more, which is greater than that caused by RF energy deposition.

3.6 Contact and induced currents

At frequencies lower than 10 MHz, where the wavelength of RF radiation is at least an order of magnitude longer than the dimensions of the human body, sources giving rise to appreciable exposures tend to be those that are in close proximity to the body and therefore at distances well within a wavelength. In such

circumstances, coupling and field behaviour inside the body are characterized by near-zone reactive fields and are quasi-static in character. The electric and magnetic fields become decoupled, and they act separately and additively inside tissue medium (Lin, 2000; 2007). The total induced fields can therefore be obtained by combining the two independent quasi-static electric and magnetic solutions of the electromagnetic field theory.

For an induced electric field E (V/m) at a point in the body, the corresponding induced current density, J (A/m^2), can be calculated through the following formula:

$$J = \sigma E \tag{3.5}$$

where σ is the electrical conductivity (S/m) of the tissue. It is then possible to integrate J over the body cross-section in vertically stacked horizontal slices in order to gain an understanding of how induced current varies with height through the body. Figure 3.4 shows an example calculation from Dimbylow (1997) at a frequency just below the body resonance (30 MHz) where the maximum layer current occurs at the feet and a frequency above resonance (120 MHz) where the maximum layer current occurs at the mid-height of the body. Note that the step at 1.1 m height arises because the current in the arms has been neglected in the calculation.

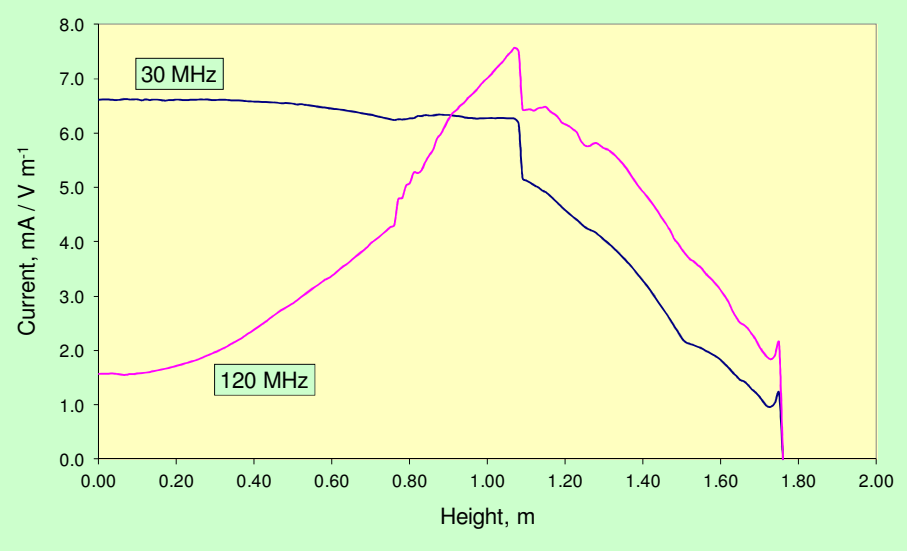

Figure 3.4. Variation of layer-averaged current with height in the body for a vertically polarized uniform field incident towards the front of the body.

The magnitude of induced currents dependents on similar factors to SAR, such as the electric and magnetic field strength, the polarization of the field, and the grounding conditions. In general, the current must reduce to zero at the top of the head, but it will not reduce to zero at the feet, especially if there is a good contact to the ground. Similarly, current may flow through and out of an arm if the hand is in electrical contact with a conducting object.

Operators of RF plastic sealers represent an occupational category that is highly exposed to RF EMFs (Wilén et al., 2004), where the induced current flowing from the feet to the ground may reach few hundreds of mA. The coupling of the body to the electric field component from these devices is usually stronger than that of the magnetic field. The existence of high electric fields around the electrodes would induce RF currents that would flow along the legs and torso. Maximum absorption occurs in the limbs (70% of the total absorbed power) where the current density, and therefore also the localised SAR, increases considerably due to a small cross section and a high amount of low-conductivity bone. Computational studies suggest that the local 10 g average SAR is about 10 W/kg for the arm and 5–8 W/kg for the foot with 100 mA current through that limb (Dimbylow, 2001; Findlay & Dimbylow, 2005). In the case of good contact with the ground the current in the lower legs, increases considerably and the maximum current density shifts to the ankles. Additionally, the whole body average SAR may increase by a factor of 2 as Chen, Gandhi and Conover (1991) have reported. Gandhi et al. (1997) suggested that other posture-related changes such as extending the hands over the electrodes of sitting may further increase the SAR by a factor of 2 or more (Gandhi et al., 1997). According to Jokela and Puranen (1999), the induced current is not affected strongly by the variation in the electric field as a function of the distance because the whole body integrates capacitive displacement current. As the distance increases, the

electric field becomes more uniform which partly compensates for the decrease of the peak field at the electrode plane.

3.7 Auditory effect

Exposure to a high peak power pulsed RF signal may result in a physiologically insignificant but rapid temperature rise leading to an auditory stimulation response in animals and humans. The effect occurs at frequencies ranging from hundreds of MHz to tens of GHz and is known as the microwave auditory (or hearing) effect (Lin, 1980; 2007; Lin & Wang, 2007). Transient localised heating during pulses leads to tissue expansion and generates an acoustic wave of pressure that travels by bone conduction to the inner ear where it activates the cochlea receptors the same way as in normal hearing. A single microwave pulse can be perceived as an acoustic click or knocking sound and a train of microwave pulses to the head can be sensed as a buzz or audible tune, with a pitch corresponding to the pulse repetition rate.

Experimental and theoretical studies have shown that the microwave auditory phenomenon does not arise from an interaction of microwave pulses directly with the auditory nerves or neurons along the auditory neurophysiological pathways of the central nervous system. Peak power densities of a few kW/m^2 are required to exceed the threshold acoustic pressure for hearing in humans (20 mPa).

The induced sound frequency exhibits an acoustically resonant behaviour where pulses appropriately separated in time are able to reinforce the pressure waves in the head, leading to increased sensitivity. The resonant frequency depends on the size of the head; the smaller the head radius, the higher the frequency. For rat-size heads, the predicted acoustic frequencies are 25 to 35 kHz in the ultrasonic range, which rats can easily hear. For the size of human heads, resonant frequencies of 7 to 15 kHz have been found which are clearly within the audible range of humans.

REFERENCES

Adair ER, Black DR (2003). Thermoregulatory responses to RF energy absorption. Bioelectromagnetics, Suppl 6:S17-S38.

Adair ER, Mylacraine KS, Allen SJ (2003). Thermophysiological consequences of whole body resonant RF exposure (100 MHz) in human volunteers. Bioelectromagnetics, 24(7):489-501.

Anderson V (2003). Comparisons of peak SAR levels in concentric sphere head models of children and adults for irradiation by a dipole at 900 MHz. Phys Med Biol, 48(20):3263-3275.

Beard B et al. (2006). Comparisons of computed mobile phone induced SAR in the SAM phantom to that in anatomically correct models of the human head. IEEE Trans Electromagn Compat, 48:397-407.

Bernardi P et al. (1998). SAR distribution and temperature increase in an anatomical model of the human eye exposed to the field radiated by the user antenna in a wireless LAN. IEEE Trans Microwave Theory Tech, 46(12):2074-2082.

Bernardi P et al. (2000). Specific absorption rate and temperature increases in the head of a cellular-phone user. IEEE Trans Microwave Theory Tech, 48:1118-1126.

Bernardi P et al. (2001). Power absorption and temperature elevations induced in the human head by a dual-band monopole-helix antenna phone. IEEE Trans Microwave Theory and Tech 49(12):2539-2546. IEEE Trans Microwave Theory Tech, 49(12):2539-2546.

Bernardi P et al. (2003). Specific absorption rate and temperature elevation in a subject exposed in the far-field of radio-frequency sources operating in the 10-900-MHz range. IEEE Trans Biomed Eng, 50(3):295-304.

Bit-Babik G et al. (2005). Simulation of exposure and SAR estimation for adult and child heads exposed to radiofrequency energy from portable communication devices. Radiat Res, 163(5):580-590.

Buccella C, De Santis V, Feliziani M (2007). Prediction of temperature increase in human eyes due to RF sources. IEEE Trans Electromagnet Compat, 49:825-833.

Cech R, Leitgeb N, Pediaditis M (2007). Fetal exposure to low frequency electric and magnetic fields. Phys Med Biol, 52(4):879-888.

Chatterjee I, Wu D, Gandhi OP (1986). Human body impedance and threshold currents for perception and pain for contact hazard analysis in the VLF-MF band. IEEE Trans Biomed Eng, 33(5):486-494.

Chen JY, Gandhi OP, Conover DL (1991). SAR and induced current distributions for operator exposure to RF dielectric sealers. EEE Trans on Electromag Compat, 33(3):252-261.

Christ A, Kuster N (2005). Differences in RF energy absorption in the heads of adults and children. Bioelectromagnetics, Suppl 7:S31-44.

Christ A et al. (2010a). Age-dependent tissue-specific exposure of cell phone users. Phys Med Biol, 55(7):1767-1783.

Christ A et al. (2010b). The Virtual Family--development of surface-based anatomical models of two adults and two children for dosimetric simulations. Phys Med Biol, 55(2):N23-38.

Cleveland RF, Jr., Athey TW (1989). Specific absorption rate (SAR) in models of the human head exposed to hand-held UHF portable radios. Bioelectromagnetics, 10(2):173-186.

Conil E et al. (2008). Variability analysis of SAR from 20 MHz to 2.4 GHz for different adult and child models using finite-difference time-domain. Phys Med Biol, 53(6):1511-1525.

Dawson TW, Caputa K, Stuchly MA (1997). A comparison of 60 Hz uniform magnetic and electric induction in the human body. Phys Med Biol, 42(12):2319-2329.

de Salles AA, Bulla G, Rodriguez CE (2006). Electromagnetic absorption in the head of adults and children due to mobile phone operation close to the head. Electromagn Biol Med, 25(4):349-360.

Dimbylow P (2005a). Resonance behaviour of whole-body averaged specific energy absorption rate (SAR) in the female voxel model, NAOMI. Phys Med Biol, 50(17):4053-4063.

Dimbylow P (2005b). Development of the female voxel phantom, NAOMI, and its application to calculations of induced current densities and electric fields from applied low frequency magnetic and electric fields. Phys Med Biol, 50(6):1047-1070.

Dimbylow P (2006). Development of pregnant female, hybrid voxel-mathematical models and their application to the dosimetry of applied magnetic and electric fields at 50 Hz. Phys Med Biol, 51(10):2383-2394.

Dimbylow P (2007). SAR in the mother and foetus for RF plane wave irradiation. Phys Med Biol, 52(13):3791-3802.

Dimbylow P, Bolch W (2007). Whole-body-averaged SAR from 50 MHz to 4 GHz in the University of Florida child voxel phantoms. Phys Med Biol, 52(22):6639-6649.

Dimbylow P, Bolch W, Lee C (2010). SAR calculations from 20 MHz to 6 GHz in the University of Florida newborn voxel phantom and their implications for dosimetry. Phys Med Biol, 55(5):1519-1530.

Dimbylow PJ (1997). FDTD calculations of the whole-body averaged SAR in an anatomically realistic voxel model of the human body from 1 MHz to 1 GHz. Phys Med Biol, 42(3):479-490.

Dimbylow PJ (2001). The relationship between localised SAR in the arm and wrist current. Radiat Prot Dosimetry, 95(2):177-179.

Dimbylow PJ (2002). Fine resolution calculations of SAR in the human body for frequencies up to 3 GHz. Phys Med Biol, 47(16):2835-2846.

Durney CH, Massoudi H, Iskander MF. Radiofrequency radiation dosimetry handbook. Fourth ed. Brooks Air Force Base, TX 78235, USAF School of Aerospace Medicine, 1986 (USAFSAM-TR-85-73).

Emery AF et al. (1975). Microwave induced temperature rises in rabbit eyes in cataract research. J Heat Transfer, 97:123-128.

Findlay RP, Dimbylow PJ (2005). Effects of posture on FDTD calculations of specific absorption rate in a voxel model of the human body. Phys Med Biol, 50(16):3825-3835.

914 Findlay RP, Lee AK, Dimbylow PJ (2009). FDTD calculations of SAR for child voxel models in different postures
915 between 10 MHz and 3 GHz. Radiat Prot Dosimetry, 135(4):226-231.

916 Flyckt VM et al. (2007). Calculation of SAR and temperature rise in a high-resolution vascularized model of the
917 human eye and orbit when exposed to a dipole antenna at 900, 1500 and 1800 MHz. Phys Med Biol,
918 52(10):2691-2701.

919 Foster KR, Adair ER (2004). Modeling thermal responses in human subjects following extended exposure to
920 radiofrequency energy. Biomed Eng Online, 28(3):4.

921 Fujimoto M et al. (2006). FDTD-derived correlation of maximum temperature increase and peak SAR in child and
922 adult head models due to dipole antenna. IEEE Trans Electromagn Compat, 48:240-247.

923 Fukunaga K, Watanabe S, Yamanaka Y (2004). Dielectric properties of tissue-equivalent liquids and their effects
924 on specific absorption rate. IEEE Trans Electromagn Compat, 46:126-129.

925 Furse CM, Gandhi OP (1998). Calculation of electric fields and currents induced in a millimeter-resolution human
926 model at 60 Hz using the FDTD method. Bioelectromagnetics, 19(5):293-299.

927 Gabriel C, Gabriel S, Corthout E (1996). The dielectric properties of biological tissues: I. Literature survey. Phys
928 Med Biol, 41(11):2231-2249.

929 Gabriel C. Dielectric properties of tissues. In: Klauenberg BJ, Miclavcic D, eds. Radio frequency radiation
930 dosimetry and its relationship to the biological effects of electromagnetic fields. Dordrecht, Kluwer Adademic
931 Publishers, 2000:75-84.

932 Gabriel C (2005). Dielectric properties of biological tissue: variation with age. Bioelectromagnetics, Suppl 7:S12-
933 18.

934 Gabriel C (2007). Tissue equivalent material for hand phantoms. Phys Med Biol, 52(14):4205-4210.

935 Gabriel S, Lau RW, Gabriel C (1996a). The dielectric properties of biological tissues: II. Measurements in the
936 frequency range 10 Hz to 20 GHz. Phys Med Biol, 41(11):2251-2269.

937 Gabriel S, Lau RW, Gabriel C (1996b). The dielectric properties of biological tissues: III. Parametric models for
938 the dielectric spectrum of tissues. Phys Med Biol, 41(11):2271-2293.

939 Gandhi OP, Lazzi G, Furse CM (1996). Electromagnetic absorption in the human head and neck for mobile
940 telephones at 835 and 1900 MHz. IEEE Trans Microwave Theory Tech, 44(10):1884-1896.

941 Gandhi OP et al. (1997). Induced current and SAR distributions for a worker model exposed to an RF dielectric
942 heater under simulated workplace conditions. Health Phys, 72(2):236-242.

943 Gandhi OP, Li QX, Kang G (2001). Temperature rise for the human head for cellular telephones and for peak
944 SARs prescribed in safety guidelines. IEEE Trans Microwave Theory Tech, 49(9):1607-1613.

945 Gandhi OP, Kang G (2002). Some present problems and a proposed experimental phantom for SAR compliance
946 testing of cellular telephones at 835 and 1900 MHz. Phys Med Biol, 47(9):1501-1518.

947 Gosselin MC et al. (2009). Dependence of the occupational exposure to mobile phone base stations on the
948 properties of the antenna and the human body. IEEE Trans Electromagn Compat, 51(2):227-235.

949 Griffiths DJ. Introduction to Electrodynamics. Second ed. New Jersey, Prentice Hall, 1989.

950 Guy AW et al. (1975). Effect of 2450-MHz radiation on the rabbit eye. IEEE Trans Microw Theory Tech,
951 23(6):492-498.

952 Hadjem A et al., eds. Influence of the ear's morphology on specific absorption rate (SAR) induced in a child head
953 using two source models. Microwave Symposium Digest, 2005 IEEE MTT-S International; 2005 12-17 June 2005.

954 Hartsgrove G, Kraszewski A, Surowiec A (1987). Simulated biological materials for electromagnetic radiation
955 absorption studies. Bioelectromagnetics, 8(1):29-36.

HCN - Health Council of the Netherlands. Influence of radiofrequency telecommunication signals on children's brains. The Hague, Health Council of the Netherlands, 2011 (2011/20E).

Hirata A, Matsuyama SI, Shiozawa T (2000). Temperature rises in the human eye exposed to EM waves in the frequency range 0.6-6 GHz. IEEE Trans Electromagn Compat, 42(4):386-393.

Hirata A, Morita M, Shiozawa T (2003). Temperature increase in the human head due to a dipole antenna at microwave frequencies. IEEE Trans Electromagn Compat, 45(1):109-116.

Hirata A, Shiozawa T (2003). Correlation of maximum temperature increase and peak SAR in the human head due to handset antennas. IEEE Trans Microw Theory Tech, 51(7):1834-1841.

Hirata A (2005). Temperature increase in human eyes due to near-field and far-field exposures at 900 MHz, 1.5 GHz, and 1.9 GHz. IEEE Trans Electromagn Compat, 47(1):68-76.

Hirata A et al. (2006). Correlation between maximum temperature increase and peak SAR with different average schemes and masses. IEEE Trans Electromagn Compat, 48(3):569-578.

Hirata A, Asano T, Fujiwara O (2007). FDTD analysis of human body-core temperature elevation due to RF far-field energy prescribed in the ICNIRP guidelines. Phys Med Biol, 52(16):5013-5023.

Hirata A, Shirai K, Fujiwara O (2008). On averaging mass of SAR correlating with temperature elevation due to a dipole antenna. Prog Electromagn Res, 84:221-237.

Hirata A, Fujiwara O (2009). The correlation between mass-averaged SAR and temperature elevation in the human head model exposed to RF near-fields from 1 to 6 GHz. Phys Med Biol, 54(23):7227-7238.

Hombach V et al. (1996). The dependence of EM energy absorption upon human head modeling at 900 MHz. IEEE Trans Microw Theory Tech, 44(10):1865-1873.

Ibrahim A et al. (2005). Analysis of the temperature increase linked to the power induced by RF source. Prog Electromagn Res, 52:23-46.

ICNIRP - International Commission on Non-ionizing Radiation Protection (1998). Guidelines for limiting exposure to time-varying electric, magnetic, and electromagnetic fields (up to 300 GHz). Health Phys, 74(4):494-522.

ICNIRP - International Commission on Non-ionizing Radiation Protection. Exposure to high frequency electromagnetic fields, biological effects and health consequences (100 kHz - 300 GHz). Vecchia P, et al., eds. Oberschleissheim, International Commission on Non-Ionizing Radiation Protection, 2009 (ICNIRP 16/2009).

ICRP - International Commission on Radiological Protection (2002). Basic anatomical and physiological data for use in radiological protection: reference values. A report of age- and gender-related differences in the anatomical and physiological characteristics of reference individuals. ICRP Publication 89. Ann ICRP, 32(3-4):5-265.

IEC - International Electrotechnical Committee (2005). Human exposure to radio frequency fields from hand-held and body-mounted wireless communication devices – Human models, instrumentation, and procedures – Part 1: Procedure to determine the specific absorption rate (SAR) for hand-held devices used in close proximity to the ear (frequency range of 300 MHz to 3 GHz) (IEC 62209-1). International Electrotechnical Committee, (http://webstore.iec.ch/webstore/webstore.nsf/Artnum_PK/33746, accessed 03-02-2014).

IEEE - Institute of Electrical and Electronics Engineers. IEEE recommended practice for measurements and computations of radio frequency electromagnetic fields with respect to human exposure to such fields, 100 kHz-300 GHz. New York, IEEE, 2002 (IEEE C95.3-2002).

IEEE - Institute of Electrical and Electronics Engineers. IEEE recommended practice for determining the peak spatial-average specific absorption rate (SAR) in the human head from wireless communications devices: measurement techniques. New York, IEEE, 2003 (IEEE 1528-2003).

IEEE - Institute of Electrical and Electronics Engineers. IEEE standard for safety levels with respect to human exposure to radio frequency electromagnetic fields, 3 kHz to 300 GHz. New York, IEEE, 2005 (IEEE C95.1-2005).

Jokela K, Puranen L (1999). Occupational RF Exposures. Radiat Prot Dosim, 83(1-2):119-124.

1000 Kainz W et al. (2003). Calculation of induced current densities and specific absorption rates (SAR) for pregnant
1001 women exposed to hand-held metal detectors. Phys Med Biol, 48(15):2551-2560.

1002 Kawai H et al. (2006). Simple modeling of an abdomen of pregnant women and its application to SAR estimation.
1003 IEICE Trans Comm, E98-B(12):3401-3410.

1004 Kawai H et al. (2010). Computational dosimetry in embryos exposed to electromagnetic plane waves over the
1005 frequency range of 10 MHz-1.5 GHz. Phys Med Biol, 55(1):N1-11.

1006 Keshvari J, Lang S (2005). Comparison of radio frequency energy absorption in ear and eye region of children
1007 and adults at 900, 1800 and 2450 MHz. Phys Med Biol, 50(18):4355-4369.

1008 Keshvari J, Keshvari R, Lang S (2006). The effect of increase in dielectric values on specific absorption rate
1009 (SAR) in eye and head tissues following 900, 1800 and 2450 MHz radio frequency (RF) exposure. Phys Med Biol,
1010 51(6):1463-1477.

1011 Kobayashi T et al. (1993). Dry phantom composed of ceramics and its application to SAR estimation. IEEE Trans
1012 Microw Theory Tech, 41(1):136-140.

1013 Kühn S et al. (2009). Assessment of induced radio-frequency electromagnetic fields in various anatomical human
1014 body models. Phys Med Biol, 54(4):875-890.

1015 Kuster N, Schönborn F (2000). Recommended minimal requirements and development guidelines for exposure
1016 setups of bio-experiments addressing the health risk concern of wireless communications. Bioelectromagnetics,
1017 21(7):508-514.

1018 Kyriakou A et al. (2012). Local tissue temperature increase of a generic implant compared to the basic restrictions
1019 defined in safety guidelines. Bioelectromagnetics, 33(5):366-374.

1020 Lagendijk JJ (1982). A mathematical model to calculate temperature distributions in human and rabbit eyes during
1021 hyperthermic treatment. Phys Med Biol, 27(11):1301-1311.

1022 Lazebnik M et al. (2005). Tissue-mimicking phantom materials for narrowband and ultrawideband microwave
1023 applications. Phys Med Biol, 50(18):4245-4258.

1024 Lee A-K, Choi H-D, Choi JI (2007). Study on SARs in head models with different shapes by age using SAM model
1025 for mobile phone exposure at 835 MHz. IEEE Trans Electromagn Compat, 49(2):302-312.

1026 Lee AK et al. (2009). Development of 7-year-old Korean child model for computational dosimetry. ETRI J,
1027 31:237–239.

1028 Lee C et al. (2006). Whole-body voxel phantoms of paediatric patients--UF Series B. Phys Med Biol, 51(18):4649-
1029 4661.

1030 Lin JC (1980). The microwave auditory phenomenon. Proc IEEE, 68(1):67-73.

1031 Lin JC (2000). Cellular mobile telephones and children. IEEE Antenn Propag M, 44(5):142- 145.

1032 Lin JC (2007). Dosimetric comparison between different quantities for limiting exposure in the RF band: rationale
1033 and implications for guidelines. Health Phys, 92(6):547-553.

1034 Lin JC, Wang Z (2007). Hearing of microwave pulses by humans and animals: effects, mechanism, and
1035 thresholds. Health Phys, 92(6):621-628.

1036 Martínez-Búrdalo M et al. (2004). Comparison of FDTD-calculated specific absorption rate in adults and children
1037 when using a mobile phone at 900 and 1800 MHz. Phys Med Biol, 49(2):345-354.

1038 Mason PA et al. (2000a). Effects of frequency, permittivity, and voxel size on predicted specific absorption rate
1039 values in biological tissue during electromagnetic-field exposure. IEEE Trans Microw Theory Tech, 48(11):2050-
1040 2058.

1041 Mason PA et al. Recent advancements in dosimetry measurements and modeling. In: Klauenberg BJ, Miclavcic
1042 D, eds. Radio frequency radiation dosimetry and its relationship to the biological effects of electromagnetic fields.
1043 Dordrecht, Kluwer Adademic Publishers, 2000b:141-155.

McIntosh RL, Iskra S, Anderson V (2014). Significant RF-EMF and thermal levels observed in a computational model of a person with a tibial plate for grounded 40 MHz exposure. Bioelectromagnetics, 35(4):284-295.

Nagaoka T et al. (2004). Development of realistic high-resolution whole-body voxel models of Japanese adult males and females of average height and weight, and application of models to radio-frequency electromagnetic-field dosimetry. Phys Med Biol, 49(1):1-15.

Nagaoka T et al. (2007). An anatomically realistic whole-body pregnant-woman model and specific absorption rates for pregnant-woman exposure to electromagnetic plane waves from 10 MHz to 2 GHz. Phys Med Biol, 52(22):6731-6745.

Neubauer G et al. (2009). The relation between the specific absorption rate and electromagnetic field intensity for heterogeneous exposure conditions at mobile communications frequencies. Bioelectromagnetics, 30(8):651-662.

Nikawa Y, Chino M, Kikuchi K (1996). Soft and dry phantom modeling material using silicone rubber with carbon fiber. IEEE Trans Microw Theory Tech, 44(10):1949-1953.

NRPB - National Radiological Protection Board. Review of the scientific evidence for limiting exposure to electromagnetic fields (0-300 GHz). Chilton, NRPB, 2004a (Doc NRPB 15(3)).

NRPB - National Radiological Protection Board. Advice on Limiting Exposure to Electromagnetic Fields (0-300 GHz). Chilton, NRPB, 2004b (Doc NRPB 15(2)).

Okano Y et al. (2000). The SAR evaluation method by a combination of thermographic experiments and biological tissue-equivalent phantoms. IEEE Trans Microw Theory Tech, 48(11):2094-2103.

Olsen RG (1979). Preliminary studies: far-field microwave dosimetric measurements of a full-scale model of man. J Microw Power, 14(4):383-388.

Olsen RG, Griner TA (1989). Outdoor measurement of SAR in a full-sized human model exposed to 29.9 MHz in the near field. Bioelectromagnetics, 10(2):161-171.

Pennes HH (1948). Analysis of tissue and arterial blood temperatures in the resting human forearm. J Appl Physiol, 1(2):93-122.

Peyman A, Rezazadeh AA, Gabriel C (2001). Changes in the dielectric properties of rat tissue as a function of age at microwave frequencies. Phys Med Biol, 46(6):1617-1629.

Peyman A et al. (2007). Dielectric properties of porcine cerebrospinal tissues at microwave frequencies: in vivo, in vitro and systematic variation with age. Phys Med Biol, 52(8):2229-2245.

Peyman A et al. (2009). Variation of the dielectric properties of tissues with age: the effect on the values of SAR in children when exposed to walkie-talkie devices. Phys Med Biol, 54(2):227-241.

Peyman A, Gabriel C (2010). Cole-Cole parameters for the dielectric properties of porcine tissues as a function of age at microwave frequencies. Phys Med Biol, 55(15):N413-419.

Razmadze A et al. (2009). Influence of specific absorption rate averaging schemes on correlation between mass-averaged specific absorption rate and temperature rise. Electromagnetics, 29(1):77-90.

Repacholi MH (1998). Low-level exposure to radiofrequency electromagnetic fields: health effects and research needs. Bioelectromagnetics, 19(1):1-19.

Schmid G, Überbacher R (2005). Age dependence of dielectric properties of bovine brain and ocular tissues in the frequency range of 400 MHz to 18 GHz. Phys Med Biol, 50(19):4711-4720.

Schönborn F, Burkhardt M, Kuster N (1998). Differences in energy absorption between heads of adults and children in the near field of sources. Health Phys, 74(2):160-168.

Sheppard AR, Swicord ML, Balzano Q (2008). Quantitative evaluations of mechanisms of radiofrequency interactions with biological molecules and processes. Health Phys, 95(4):365-396.

Stolwijk JAJ, Hardy JD. Control of body temperature. In: Douglas HK, ed. Handbook of physiology: a critical, comprehensive presentation of physiological knowledge and concepts. Section 9: Reactions to environmental agents. Bethesda, MD, American Physiology Society, 1977:45-69.

Stuchly MA et al. (1987). RF energy deposition in a heterogeneous model of man: near-field exposures. IEEE Trans Biomed Eng, 34(12):944-950.

Tavlove A, Hagness SC. Computational electrodynamics: the finite-difference time-domain method. Third ed. Norwood, MA, Artech House, 2005.

Thurai M et al. (1984). Variation with age of the dielectric properties of mouse brain cerebrum. Phys Med Biol, 29(9):1133-1136.

Thurai M et al. (1985). Dielectric properties of developing rabbit brain at 37 degrees C. Bioelectromagnetics, 6(3):235-242.

Tinniswood AD, Furse CM, Gandhi OP (1998). Power deposition in the head and neck of an anatomically based human body model for plane wave exposures. Phys Med Biol, 43(8):2361-2378.

Togashi T et al. (2008). FDTD calculations of specific absorption rate in fetus caused by electromagnetic waves from mobile radio terminal using pregnant woman model. IEEE Trans Microw Theory Tech, 56(2):554-559.

Uusitupa T et al. (2010). SAR variation study from 300 to 5000 MHz for 15 voxel models including different postures. Phys Med Biol, 55(4):1157-1176.

van Leeuwen GM et al. (1999). Calculation of change in brain temperatures due to exposure to a mobile phone. Phys Med Biol, 44(10):2367-2379.

Vermeeren G et al. (2008). Statistical multipath exposure of a human in a realistic electromagnetic environment. Health Phys, 94(4):345-354.

Wainwright P (2000). Thermal effects of radiation from cellular telephones. Phys Med Biol, 45(8):2363-2372.

Wainwright PR (2003). The relationship of temperature rise to specific absorption rate and current in the human leg for exposure to electromagnetic radiation in the high frequency band. Phys Med Biol, 48(19):3143-3155.

Wainwright PR (2007). Computational modelling of temperature rises in the eye in the near field of radiofrequency sources at 380, 900 and 1800 MHz. Phys Med Biol, 52(12):3335-3350.

Wang J, Fujiwara O (1999). FDTD computation of temperature rise in the human head for portable telephones. IEEE Trans Microw Theory Tech, 47(8):1528-1534.

Wang J, Fujiwara O (2003). Comparison and evaluation of electromagnetic absorption characteristics in realistic human head models of adult and children for 900-MHz mobile telephones. IEEE Trans Microw Theory Tech, 51(3):966-971.

Wang J et al. (2006). FDTD calculation of whole-body average SAR in adult and child models for frequencies from 30 MHz to 3 GHz. Phys Med Biol, 51(17):4119-4127.

WHO - World Health Organization. Electromagnetic fields (300 Hz to 300 GHz). Geneva, World Health Organization, 1993.

Wiart J et al. (2008). Analysis of RF exposure in the head tissues of children and adults. Phys Med Biol, 53(13):3681-3695.

Wilén J et al. (2004). Electromagnetic field exposure and health among RF plastic sealer operators. Bioelectromagnetics, 25(1):5-15.

Youngs IJ et al. (2002). Design of solid broadband human tissue simulant materials. IEE Proc Sci Meas Tech, 149(6):323-328.